

Case Report

Low-Cost Syngas Shifting for Remote Gasifiers: Combination of CO₂ Adsorption and Catalyst Addition in a Novel and Simplified Packed Structure

Ricardo A. Narváez C. ^{1,2,3,*} , Richard Blanchard ³ , Roger Dixon ⁴, Valeria Ramírez ¹  and Diego Chulde ¹

¹ Instituto Nacional de Eficiencia Energética y Energías Renovables (INER), Quito EC170507, Ecuador; valeria.ramirez@iner.gob.ec (V.R.); diego.chulde@iner.gob.ec (D.C.)

² Facultad de Ingeniería Química, Universidad Central del Ecuador, Quito EC170521, Ecuador

³ Centre for Renewable Energy Systems Technology (CREST), Wolfson School Mechanical, Manufacturing and Electrical Engineering, Loughborough University, Loughborough LE11 3GR, UK; r.e.blanchard@lboro.ac.uk

⁴ Wolfson School Mechanical, Manufacturing and Electrical Engineering, Loughborough University, Loughborough LE11 3TU, UK; r.dixon@lboro.ac.uk

* Correspondence: ricardo.narvaez@iner.gob.ec; Tel.: +593-2-393-1390

Received: 27 December 2017; Accepted: 26 January 2018; Published: 1 February 2018

Abstract: This paper presents the technical validation of a novel, low-complexity alternative based on the inclusion of a patented (IEPI-MU-2016-185) packed bed for improving the performance of remote, small-scale gasification facilities. This study was carried out in an updraft, atmospheric-pressure gasifier, outfitted with a syngas reflux line, air and oxygen feed, and an upper packed-bed coupled to the gasification unit to improve the syngas quality by catalytic treatment and CO₂ adsorption. The experimental facility is located in the rural community San Pedro del Laurel, Ecuador. Gasification experiments, with and without packed material in the upper chamber, were performed to assess its effect on the syngas quality. The assessment revealed that the packed material increases the carbon monoxide (CO) content in the syngas outlet stream while carbon dioxide (CO₂) was reduced. This option appears to be a suitable and low-complexity alternative for enhancing the content of energy vectors of syngas in gasification at atmospheric pressure since CO/CO₂ ratios of 5.18 and 3.27 were achieved against reported values of 2.46 and 0.94 for operations which did not include the addition of packed material. It is concluded that the upper packed-bed is an active element able to modify syngas characteristics since CO₂ content was reduced.

Keywords: biomass; municipal solid waste; gasification; syngas shifting

1. Introduction

Gasification is recognized as a suitable and promising technology for exploiting carbon-based resources (fossil or renewables) under environmentally favourable conditions, such as greenhouse gas (GHG) reduction [1–4] and high energy conversion rates [5]. Moreover, this technology offers significant opportunities for rural electrification, since it enables the optimal use of local and bio-based energy, while promoting the active participation of local stakeholders [6–8]. In such conditions, it is relevant to explore proper alternatives for optimizing the integration of local energy resources in order to reduce the implementation and operation cost of small-scale energy systems [9].

Reported options for achieving a high conversion in gasifiers imply the use of relatively complex systems, such as additional reforming units or air separators; moreover, these alternatives also require an additional investment related to their implementation. Despite their effectiveness, their complexity and relative implementation cost may not be compatible with isolated, small-scale gasification systems

that also require performance improvement. Common auxiliary services in gasifiers, for instance, air-separation units, water-gas shifting (WGS) reactors, or reformers, can be significant in the total cost of a gasification facility. Their relative costs calculated from reported direct capital costs are 1.09, 0.48, and 1.22, respectively, when compared with the cost of the gasification unit that is the comparison parameter (cost factor = 1) [10].

Regarding operational issues, auxiliary units such as those for gas compression in fluidized-bed units are the leading energy consumption concern for these type of reactors [11]. Even if such kinds of experimental components can improve the syngas quality, they are usually more expensive than commercial models [12]. Hence, seeking alternatives aimed at reducing the cost syngas improvement is a relevant topic for making the technology available for the final stakeholder. Concerning the techno-economic point of view, it is possible to affirm that low-cost and straightforward syngas shifting proposals are relevant for consolidating the cost-effectiveness of gasification. Improving syngas quality is a relevant issue for small-scale energy systems, since electricity generation is quite sensitive to fuel gas quality [13]. Moreover, efficiency is one of the factors that determine the final cost of electricity in such types of systems [14].

Although including syngas reforming (chemical processes) or carbon capture (physical processes) increases the implementation costs of a gasification-based energy system, cost-effectiveness could be achieved once the technology is scaled up [15], which may not be applicable in remote gasification systems. However, it is also noted that gasifiers without additional equipment are suitable for small-scale use, due to their simplicity and low cost. Hence, it is relevant to find syngas improvement options able to combine simplicity, effectiveness, and inexpensiveness.

Regarding other available alternatives for enhancing the syngas quality such as CO₂ or N₂ capture, it can be seen that they can raise the efficiency of downstream elements, including generator or chemical reactors, due to the reduction of gas transportation/handling capacities. Even though carbon capture appears as an emerging, yet not wholly mature, concept in energy systems, post-combustion CO₂-removal systems that are based on absorption and adsorption seem to be the most common alternatives to avoid extensive modifications of the infrastructure already implemented [16]. Despite this affirmation, pre-combustion CO₂ capture, which requires gasification, has not yet been discarded, and its combination with other pre-treatment stages could be relevant [17]. In addition, gasification technology could be significant for municipal solid waste (MSW) treatment, for instance, since it can operate despite considerable variations in the feedstock composition [18].

This work describes a novel alternative for increasing the CO/CO₂ of syngas based on CO₂ adsorption combined with WGS (a combination of physical and chemical phenomena). The patented proposal considers that both techniques handle similar operating conditions to ease their coupling. In this case, both phenomena were induced in a single structure that encloses the CO₂ adsorption and the catalysed chemical reactions [19].

It has been reported that WGS processes require a temperature range that is dependent on the catalyst; hence, it is necessary to reach proper operating conditions in order to enable the catalytic activity. In such a context, high- and low-temperature conditions could be equally exploited by selecting the proper catalyst. For instance, high-temperature WGS has been reported in the range of 350–500 °C for Fe/Cr catalyst, while low temperature ranges (150–300 °C) are appropriate for Cu/Zn catalyst operation [20]. This parameter could be close to 350 °C for Pd-Ag catalysts [21], 500 °C for Ni-Mg-Al-Ca catalysts [22], or in the range between 300 °C and 450 °C for Co-Mo catalysts [23]. Ranges between 180 °C and 300 °C for Ni-Ce-based catalysts have also been reported [24]. Nevertheless, according to [25], WGS is possible at 150 °C with Cu-ZnO-Al₂O₃ catalysts. On the other hand, CO₂ capture over zeolite at atmospheric pressure has been achieved with Zeolite 13X, which has been recognised as a suitable adsorbent, since it removes 20.1% of CO₂ at 25 °C and 1 bar [26].

Catalyst supported over zeolite could have adsorbing activity in addition to its primary function of boosting WGS; moreover, it can find application in reducing potential CO₂ emissions. Hence, it is possible to suggest that adsorption is the most compatible CO₂ capture technology in cases where

reforming is suitable. The current analysis evaluates both effects in a pilot-scale updraft gasifier equipped with an upper chamber filled with zeolite-based packed material. The analysis of syngas composition and its comparison with reported gasification systems were the evaluation parameters.

In the current work, quality criterion is based on the relative amount of CO₂ in the syngas stream. The presence of CO₂ is undesirable in fuel gases, since it implies a reduction in the global energy content [27]. However, in gasification, CO₂ is a resulting element of oxidation, and can deliver energy for reduction reactions, such as hydrogen formation. Additionally, the heat produced during its formation allows gasification temperatures above 1000 °C, which boosts the formation of CO [28]. Unlike CO₂, CO can be oxidised to deliver energy, and it is recognized as one of the components of syngas that can act as an energy carrier.

Hence, CO₂ content requires being controlled due to the multiple effects that its formation can cause on the performance of a gasifier. Moreover, it should be compared with CO, since its composition could decrease when the amount of CO₂ increases [29]. The CO/CO₂ ratio has been considered to be an indicator of the direction that an oxidation process takes between gasification and combustion [30], and as a suitable variable for controlling tasks in gasifiers [31]. The objective of this research is to present an alternative for improving atmospheric gasifiers' performance based on CO₂ adsorption and WGS, maintaining low complexity for construction and operation by inducing both phenomena in a single structure. The presented alternative is expected to become a suitable solution for small-scale gasification systems that generally require the improvement of their energy performance in order to reduce the final energy cost.

2. Materials and Methods

The experimental facility is a pilot-scale device consisting of a thermally isolated updraft gasifier equipped with an upper chamber. This chamber was filled with packed, adsorbing-catalytic material for assessing its performance. In addition to forming a gas reactor that hosts chemical reactions, this packed bed can also act as a CO₂ adsorption facility because of its use of zeolite, as described below in this section. The catalytic material is based on acid-activated Raney nickel as the active component, supported over zeolite. This material was selected based on its effectiveness and stability [32,33]. Additionally, zeolite was chosen as the support material due to its properties as a molecular sieve for CO₂ adsorption [34,35]. The gasifier is equipped with a control system that allows the CO/CO₂ ratio to be maintained during operation.

The packed-bed configuration is applied in unit operations and chemical reactions engineering as a relatively simple solution for increasing the superficial contact that is demanded by specific physical and chemical phenomena, such as adsorption and catalytic processes. Since packed beds are commonly formed by bulk solids, they allow having empty spaces surrounding the solid structures that offer the superficial contact. During industrial operations, such empty spaces are occupied by working fluids while they pass through the packed-bed structure. Moreover, the contact between the solid surfaces and the working fluids is generated. In this case, the zeolite-based material that composes the upper packed bed has been provided with active catalytic material along its surface. Moreover, it has also been put through a surface preparation process for activating potential adsorption properties of zeolite. In consideration of this, the upper packed bed is expected to host physical and chemical phenomena that increase the energy vector contents in the syngas.

Regarding the gasifier configuration, the system scheme is presented in Figure 1. It includes an inlet point for the biomass feedstock (1) located in the lower part of the packed-bed chamber (2). Biomass feedstock is added to the gasifier by a screw-type automatic solid feeder. An air inlet point (3) in the lower part of the gasification throat, and an oxygen inlet point connected to a liquid O₂ vessel (4) are also part of the research facilities for evaluating the effect of the oxygen input on the reactor performance. The gasifier is also equipped with a gas reflux pipeline (5) that can re-inject reformed syngas to the lower part of the gasification throat for modifying the gas retention time. The reduction zone temperature and the temperature in the lower part of the packed bed were registered with K-type

thermocouples. The general characteristics of the experimental facilities are stated in Table 1. Gaseous compound concentrations (O_2 , CO, CO_2 , CH_4 , and H_2) were registered with a NOVA[®] 975A in-line gas analyser (NOVA ANALYTICAL SYSTEMS[®], Hamilton, ON, Canada). In addition, an overall image of the experimental facility is presented in Figure 2.

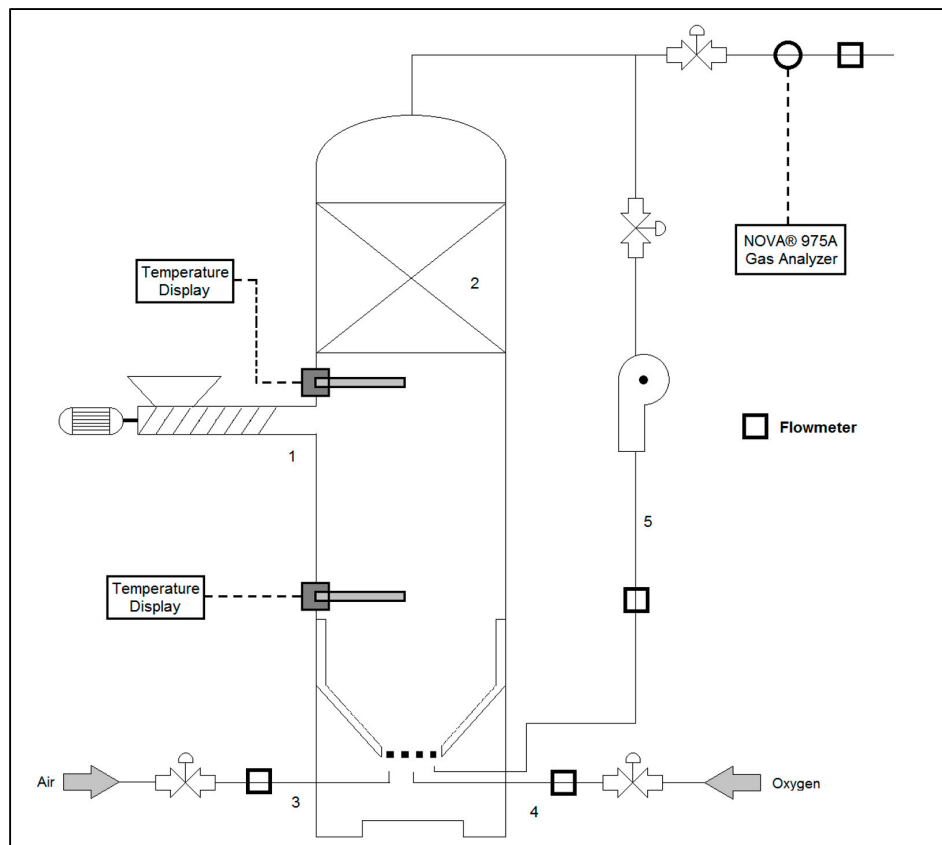


Figure 1. Gasification facility scheme.

Table 1. Characteristics of the gasification facilities.

Feeding Capacity ($kg \cdot h^{-1}$)	Diameter (mm)	Height (mm)	Throat Inclination (Degrees Taken from the Vertical Axis)	Throat Height (mm)	Throat Lower Diameter (mm)	Throat Upper Diameter (mm)
Up to 50	760	3040	43	200	260	533

The experiments consisted of performing continuous operation of the gasifier in order to gather the syngas quality information once steady-state conditions had been achieved. Unvarying conditions were ensured by implementing a 20-h stabilization period, and the experiments were designed to last 90 min without significant variations in the monitored operating variables. The gasifier operates in atmospheric pressure ranges.

Two types of experiments were carried out in steady-state conditions in order to assess the effect of packed-bed material under different oxygen contents. The first one utilized only air as the oxidizing agent, and the second one, air was combined with highly-concentrated oxygen. Each experiment was repeated three times in order to ensure their repeatability.

All experiments were performed with and without the inclusion of the packed material in the upper chamber to assess its effect. The first set of experiments was developed by using a blend of oxygen (99% *v/v* O_2) and air. The second round of experiments was carried out exclusively with ambient air. Biomass feed rate and reflux flow rate were maintained under similar conditions.

The assays considered the operating conditions in Table 2 and, moreover, thermal images of the upper chamber were registered to complement the temperature measurement



Figure 2. Gasification facility image.

Table 2. Operational variables for the experiments carried out with a blend of oxygen and ambient air.

Variable	Air Flow Rate (dm ³ ·s ^{−1})	Oxygen Flow Rate (dm ³ ·s ^{−1})	Reflux Ratio	Biomass Flow Rate (kg h ^{−1})	Packed Material Added (kg)
O ₂ + air (no packed material)	2.40	0.95	0.8	16	0.0
Only air (no packed material)	3.57	0.00	0.8	16	0.0
O ₂ + air (with packed material)	2.40	0.95	0.8	16	88.7
Only air (with packed material)	3.57	0.00	0.8	16	88.7

The configuration of the gasifier takes account of the fact that gasification performed in counter-current (as in updraft gasifiers) implies that the drying, pyrolysis, and gasification stages are clearly differentiated by the vertical temperature profile achieved during operation. Moreover, the contact between gaseous and solid phases favours the formation of energy vectors that are mainly generated through endothermic reactions [36]. A description of the chemical reactions that compose the gasification process is presented in Table 3. It is recognised that the operation generates a temperature gradient from the reduction zone (high temperature) to the upper part of the packed bed

(low temperature). Such a phenomenon is caused by the heat exchange between the ascending syngas and the descending solid biomass. Hence, the location of the packed bed is expected to exploit catalytic and CO₂ adsorption processes that occur at low temperatures in order to improve the syngas quality.

Table 3. Gasification reactions description (Extracted from [36,37]).

Stage/Phenomenon	Chemical Reaction	Heat of Reaction (kJ·g·mol ^{−1})
Drying	$\text{Biomass}_{\text{wet}} \rightarrow \text{Biomass}_{\text{dry}} + \text{H}_2\text{O}$	>0
Pyrolysis	$\text{Biomass}_{\text{dry}} \rightarrow \text{Char} + \text{Tar} + a\text{H}_2\text{O} + b\text{CO} + c\text{CO}_2 + d\text{H}_2 + e\text{CH}_4$	<0
Gasification	$\text{C} + 0.5\text{O}_2 \rightarrow \text{CO}$	−110.6
	$\text{C} + \text{O}_2 \rightarrow \text{CO}_2$	−393.8
	$\text{C}_x\text{H}_y + 0.5x\text{O}_2 \rightarrow x\text{CO} + 0.5y\text{H}_2$	<0
	Boudouard reaction $\text{C} + \text{CO}_2 \rightarrow 2\text{CO}$	172.6
	Steam gasification $\text{C} + \text{H}_2\text{O} \rightarrow \text{CO} + \text{H}_2$ $\text{C} + 2\text{H}_2\text{O} \rightarrow \text{CO}_2 + 2\text{H}_2$ $\text{C}_x\text{H}_y + x\text{H}_2\text{O} \rightarrow x\text{CO} + (x + 0.5y)\text{H}_2$	131.4
		87.2
		>0
	Methanation and reforming $\text{C} + 2\text{H}_2 \rightarrow \text{CH}_4$ $\text{CH}_4 + \text{H}_2\text{O} \rightarrow \text{CO} + 3\text{H}_2$	−74.9
		201.9

Regarding the bulk material used for the upper packed bed, it is worth mentioning that the average particle size was 0.75 cm and was mainly composed of zeolite particles previously prepared by catalytic material impregnation (Raney nickel) and thermal activation. During the experimental assays, the temperature of the syngas that reaches the lower part of the packed bed was also registered with the purpose of verifying if this condition is appropriate for the catalytic and CO₂ adsorption phenomena.

Concerning the feedstock blends prepared for the experiments, it should be mentioned that co-gasification between MSW and charcoal was proposed with the aim of exploiting the presence of MSW humidity as a water steam source. In such a context, the purpose of adding a significant proportion of a dry fuel, such as charcoal, is to ensure water evaporation inside the gasification reactor. Operating with blends of MSW and charcoal aims to obtain more significant syngas calorific values. Such an effect has been reported, since co-gasification allows improvement of the syngas quality due to the combination of volatiles and water steam in the gas phase, during gasification [38].

Feedstocks with considerable humidity and volatile carbon content (suitable for tar generation) can be combined with feedstocks with high fixed carbon content (characterized by more significant heating values and significant content of reactants proper for reduction reactions) with the purpose of enhancing the tar conversion into syngas [39]. In addition, wet-basis humidity in MSW can behave as steam at reaction conditions and react with carbonous surfaces to boost hydrogen production, as in steam gasification [40–42]. Samples were prepared with an optimal 3:2 mass proportion (charcoal and MSW), correspondingly. This figure was chosen with the purpose of maximizing the energy vector content in syngas [38,43,44].

Biomass feedstock batches were prepared by blending chopped MSW and vegetable charcoal made of palm oil kernel shell. Particle size was fixed at approximately 1 cm effective diameter. This particle size was selected since it has been reported to increase syngas yield (3.2%) and cold gas efficiency (CGE) (3.4%) during gasification, if compared to larger diameters [4]. The feedstock for these assays (MSW) was obtained from the rural community San Pedro del Laurel, Ecuador, which is a place that would benefit from the implementation of the gasification facility. MSW was sampled according to the standard method NT ENVIR 001 [45]. Proximate and ultimate analyses of batch samples were performed in all cases with standard laboratory methods.

Even if different biomass characteristics are expected to affect the output properties after a thermal decomposition process [46], it is also possible to achieve homogenous properties for the output products by controlling the operation variables [40]. Results were compared with reported figures of different gasification facilities found in the literature.

The laboratory tests performed as part of this research followed the standard procedures listed in Table 4, together with the laboratory equipment.

Table 4. Laboratory equipment required for biomass tests.

Biomass Property	Standard Code	Main Laboratory Equipment
C, H, N, S in biomass	ASTM D3176-15	PerkinElmer© 2400 Series II CHNS/O Elemental analyser
Dry-basis humidity	BS EN ISO 18134-1:2015	Memmert© SN 55 incubator
Ashes content	ASTM E1755-01(2015)	Thermo Scientific© F48000 muffle furnace
Volatile carbon content	ASTM E872-82(2013)	
Fixed carbon	-	
Gross calorific value	BS EN ISO 18125:2017	IKA© Calorimeter System C 2000

3. Results

As was mentioned, the test feedstock was composed of vegetable charcoal and MSW. Considering MSW can contain several components suitable for being differentiated by primary sorting, this initial activity was undertaken, and the results are reported in Table 5.

Table 5. MSW composition (sorted by type, wet basis).

Component	Average Value
Plastic (% wt)	11.99 ± 2.65
Paper (% wt)	11.33 ± 3.22
Kitchen waste (% wt)	76.69 ± 2.92
Humidity _{wet-basis} (% wt)	45.63 ± 2.19

Sorting results show that kitchen waste is the dominant component in MSW. Regarding proximate and ultimate composition, the data generated for MSW and kernel shell charcoal are presented in Tables 6 and 7, respectively. Data obtained from the literature is used for the purpose of comparison.

Table 6. Proximate analysis results for MSW and kernel shell charcoal (dry-basis).

Parameter	Value ¹						
	MSW _{dry-basis}	KSC	Blend (Calculated)	OPF [47]	AS [48]	PSP [49]	CSP [49]
Humidity (% wt)	4.57 ± 1.98	5.30 ± 1.66	5.01	-	-	7.82	11.76
Volatile carbon (% wt)	85.07 ± 5.48	30.99 ± 10.82	52.62	85.1	71.7	80.52	62.95
Fixed carbon (% wt)	0.90 ± 0.50	42.82 ± 11.35	24.85	11.5	19.5	10.73	18.55
Ashes (% wt)	12.47 ± 6.92	20.89 ± 5.13	17.52	3.4	1.1	0.93	6.74

¹ KSC: kernel shell charcoal, OPF: oil palm fronds, AS: almond shells, PSP: pine sawdust pellets, CSP: cotton stalk pellets.

Table 7. Ultimate analysis results for MSW and kernel shell charcoal (dry-basis).

Parameter	Value						
	MSW	KSC	Blend (Calculated)	OPF [47]	AS [48]	PSP [49]	CSP [49]
C (% wt)	75.68 ± 1.68	59.15 ± 2.36	65.76	42.4	48.9	46.11	41.65
H (% wt)	8.38 ± 0.05	4.69 ± 0.11	6.17	5.8	6.2	6.13	2.34
N (% wt)	4.36 ± 0.69	4.34 ± 0.47	4.35	3.6	0.18	0.87	0.82
S (% wt)	0.88 ± 0.08	0.36 ± 0.02	0.57	-	0.026	0.07	0.17
O (% wt) (Calculated)	13.20 ± 2.49	29.31 ± 2.52	23.16	48.2	43.5	38.07	36.52
Gross heating value (MJ·kg ⁻¹)	15.77 ± 0.19	28.85 ± 0.11	23.62	-	-	-	-
Net heating value (MJ·kg ⁻¹)	14.33	27.41	22.18	-	-	18.49	15.43

Results of the experimental assays are presented in Table 8. The figures present cold gas efficiency (CGE) values as well. This factor relates the inlet feedstock heating value with the outlet syngas heating value for explaining the thermal efficiency of the process [50].

Table 8. Average dry-basis syngas composition obtained from experimental assays.

Results	Packed Material Added		No Packed Material	
	Oxidant Gas		Oxidant Gas	
	Oxygen + Air	Air	Oxygen + Air	Air
O ₂ (% v/v)	6.89 ± 0.24	2.25 ± 0.17	11.24 ± 0.48	5.99 ± 0.68
CO (% v/v)	37.73 ± 0.63	26.39 ± 3.93	29.01 ± 7.20	12.92 ± 3.35
CO ₂ (% v/v)	7.28 ± 0.85	8.07 ± 0.76	11.80 ± 2.92	13.78 ± 2.41
CH ₄ (% v/v)	1.14 ± 0.01	0.83 ± 0.03	2.96 ± 0.24	4.27 ± 1.07
H ₂ (% v/v)	10.82 ± 1.05	7.56 ± 1.37	8.30 ± 1.75	6.21 ± 1.89
Calculated net heating value (MJ·kg ⁻¹)	7.70	5.23	6.24	3.79
Syngas output (kg·h ⁻¹)	28.89 ± 2.65	25.18 ± 2.91	28.63 ± 2.44	24.75 ± 3.04
Gaseous-phase retention time (min ⁻¹)	6.2	7.2	6.6	7.6
CGE (%)	63.96	37.34	51.34	26.30

To compare syngas compositions with reported data from literature sources, data were homogenised to a nitrogen-free basis, and the CO/CO₂ figures were calculated. The values are presented in Table 9.

Even if the packed bed activity is considered to be a relevant research topic by itself, in addition to its study in the context of the gasification case presented, thermal images were recorded reflecting the upper temperature range in order to show any potential activity to be reported. Thermal images of the upper chamber during O₂ + air operation (front and side) with packed material addition are shown in Figure 3.

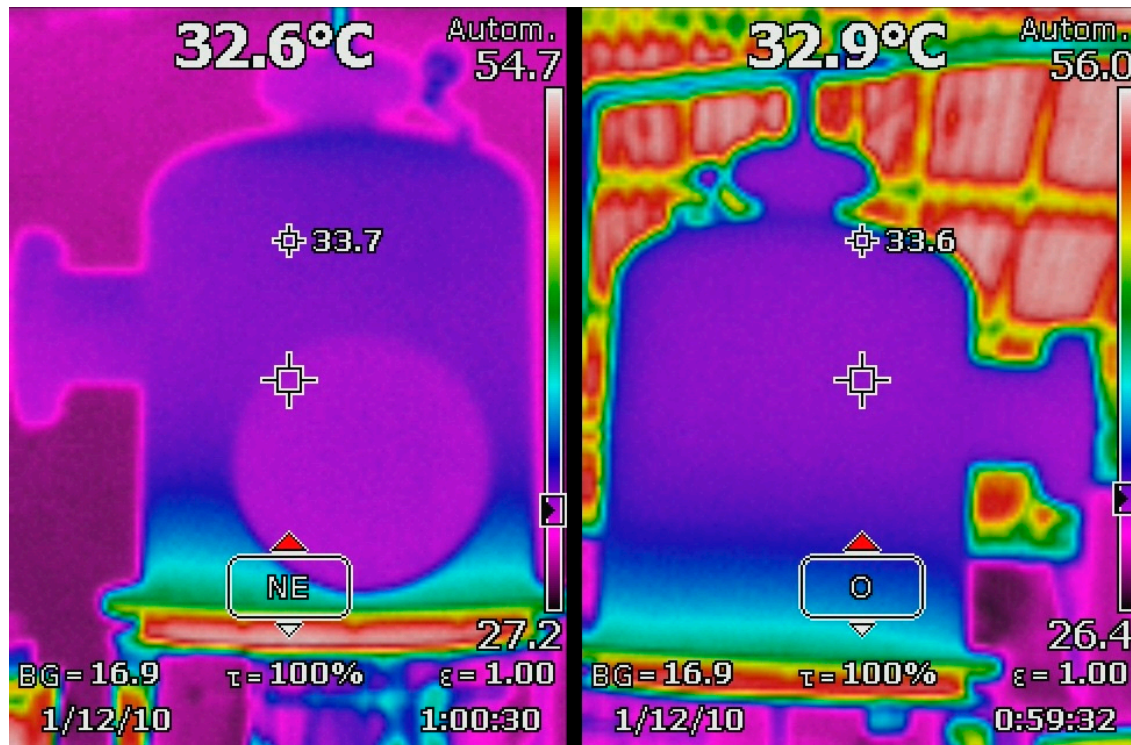


Figure 3. Thermal images of the upper chamber during O₂ + air operation with packed material addition.

Table 9. Syngas composition, CO/CO₂ ratio, and operational temperature comparison.

Parameter	Experimental Conditions				Data Reported in Literature			
	Packed Material Added		No Packed Material		OFP + Air (Calculated from [47])	AS + Steam [48]	PSP + O ₂ (Calculated from [49])	CSP + O ₂ (Calculated from [49])
	O ₂ + air	Air	O ₂ + air	Air				
T _{Reducton zone} (°C)	674	513	668	531	510	800–815	900	920
T _{Upper chamber} (°C)	128	113	122	108	-	-	-	-
O ₂ ER ¹	0.11	0.11	0.11	0.11	0.44	-	-	0.21
O ₂ (% v/v)	10.79	4.99	17.75	13.88	-	-	0.35	0.36
CO (% v/v)	59.08	58.51	45.82	29.93	45.28	24	35	38
CO ₂ (% v/v)	11.40	17.89	18.64	31.92	16.98	26	22	21
CH ₄ (% v/v)	1.79	1.84	4.68	9.89	5.66	10	3.3	2.7
H ₂ (% v/v)	16.94	16.76	13.11	14.38	20.75	39	36	36
CO/CO ₂	5.18	3.27	2.46	0.94	2.7	0.9	1.6	1.8

¹ O₂ Equivalence Ratio.

The implementation cost figures are presented for the purpose of comparing the economic incidence of this alternative if compared with other syngas enhancement methods. Even if the figures were obtained in a pilot facility, relative cost factors are shown in Table 10. It is relevant to mention that such figures, in the case of implementation costs, were obtained from the construction report carried out during the building stage of the experimental gasification facility. Since the upper chamber and the remaining parts of the gasification reactor have similar structures, the cost factors were obtained by using unit costs and relative dimensions. The baseline cost (cost factor = 1) refers to the gasifier without the upper chamber required for implementing the shifting proposal.

Table 10. Relative cost factors of gasifiers with packed-bed chamber included.

Component	Description	Regular Operation	Proposed Syngas Shifting Operation
Gasifier	The cost factor is related to the additional investment cost implied by having the upper chamber for the packed bed.	1.000	1.043
Air-mode operation	The cost factor is calculated by considering the worker-hours required for preparing the zeolite-based material and charging/discharging tasks related to its allocation. In addition, the costs of implements such Nickel-Raney, raw zeolite, activated zeolite and energy are also considered in the cost factor.	1.000	1.029
O ₂ + air-mode operation	In this case, the operation cost considers the O ₂ supply contribution in addition to the components mentioned above.	1.080	1.109

In the case of the operating costs, the variation in the cost factor is calculated by considering additional worker-hours, plus supplies required for preparing the packed material.

4. Discussion

Regarding the solid fuel that is used in these assays, a certain similarity with other reported figures can be noticed. Even if kitchen waste is not the only component of MSW, in this case, several properties of MSW, such as volatile carbon, are similar to the reported values of other types of biomass with a single component. In contrast, MSW presents a low fixed carbon content. Hence, it requires being blended with charcoal to improve its performance as fuel [43,44]. In this case, the charcoal stream is 1.5 times greater than the humid MSW and 18.13% of the total solid input was composed of free water in such conditions. Hence, the energy input contributed by the charcoal exceeds 37 times the energy requirement that the free water would require for evaporating. These figures show that it is possible to consider that evaporation was, indeed, one of the phenomena involved in gasification during the registered assays. Moreover, such consideration supports the consideration adopted about neglecting drying-type pre-treatment stages in MSW gasification. The presented figures show that co-gasification is a suitable alternative for MSW since it enables its embedded water to be used as one of the reactants, rather than as a component to be removed.

In addition, fuel-processing figures could be related to the water contained in the inlet solid fuel. Steam co-gasification processes are commonly associated with significant hydrogen production rates and with the presence of significant amounts of fixed carbon [51]. Therefore, it is expected to generate proper conditions for exploiting the water presence by adding charcoal and wet biomass blends instead of considering pre-treatment stages based on drying. The effect of avoiding this type of pre-treatment is in accord with this consideration, and has been reported for other types of organic materials, such as rubber [52]. In this case, the combination is expected to demonstrate the suitability of considering local MSW as a proper energy source to be converted in the gasifier. Steam gasification and

methane reforming processes consider water steam as one of the reactants together with solid carbon and gaseous methane, correspondingly. Moreover, it has been affirmed that this type of gas-phase reaction is the one that generates the most significant hydrogen production rate [38].

Concentrated oxygen addition increases the partial pressure of this component in the reacting gas stream, which also reduces the partial pressure of inert gases during gasification, such as nitrogen. Even if air can act as an oxidising agent, O₂ addition is expected to reduce heat losses due to inert gases heating, and to increase the reaction rate due to the augmentation of the concentration of one of the reactants. Both effects can increase gasification temperature; hence, H₂ and CO formation can be boosted in comparison with gasification fed with air only. Similar effects of adding O₂ have been reported previously [53].

The design of the gasifier coupled an initial gasification stage formed by an updraft configuration with gas treatment in series. The gas treatment was specifically designed to improve the syngas quality, i.e., to increase the content of energy vectors, such as H₂, CO, and CH₄. Accepting that enhancing the energy vectors contents in the syngas is a suitable treatment to improve the gasifier's performance, it should be mentioned that a packed-bed able to host catalytic processes and carbon capture related to CO₂ appears to be a suitable alternative when compared with other gas-shift options. The presence of the packed-bed allowed the achievement of promising figures related to syngas quality compared with other proposals with the same aim.

Even if the lower part of the gasifier initiated the solid-gas conversion, as was verified by the high temperature recorded, an extra stage for gas reforming and CO₂ retention was also considered in order to enhance syngas quality. Both effects were induced in the same packed bed by putting the catalytic material over a support base that can accomplish this primary purpose together with CO₂ adsorption. Despite the fact that generating a heterogeneous behaviour along a single structure such as a packed bed could be a non-desirable effect (CO₂ adsorption with molecular sieve and catalysed chemical changes are mutually exclusive surface phenomena, and are planned to occur in different zones of the same packed-bed), the construction and operation of an atmospheric gasifier coupled with a packed-bed structure is, a priori, more accessible than a pressurized gasifier case. If both technological alternatives could deliver similar outputs, it would be expected that avoiding high-pressure conditions would result in a low-complexity option.

The comparative analysis of results shows that the chemical phenomenon can be achieved by inducing effects such as gas retention time growth by the presence of a porous medium, and also due to the catalytic activity provided by the active material adsorbed over its surface (Raney nickel) [54,55]. The occurrence of the chemical phenomena responsible for the gaseous compounds reforming was generated by the presence of the nickel-based catalyst [56], and boosted by the physical effects induced by the porous media (gas retention time increase and augmentation of the interfacial area exposed to the catalyst), as has been verified in packed-bed reactors.

Additionally, it can be confirmed that wet MSW co-gasification enhances hydrogen formation even if feedstock composition is variable. This is shown by the relatively high figures for the standard deviation of all proximate analysis components when compared with the reported results of experiments carried out with fixed types of biomass and assumed low variability in their composition figures. The statement is also supported by the fact that hydrogen content was significant, although the ultimate composition of this element in feedstock was relatively low. Accepting that MSW is a poor feedstock material in terms of quality compared with other bio-based materials such as the ones used in this work for comparison purposes, the validation of the above-presented technology could be assessed with a more suitable solid fuel in order to reduce the test differences related with the inputs.

Although the effect of the presence of the packed bed in syngas does indeed show an improvement in its quality, it is necessary to determine the predominant phenomenon that leads to achieving this outcome. Even if the catalytic activity is recognised as a reduction of the activation energy of a chemical reaction and it can be verified by the increase of chemical conversion rate [57], effectiveness, efficiency, and cost are recognised as the selection criteria [58]. Although Raney nickel was used

in this work due to its cost effectiveness and availability, it is suitable to be reproduced with other catalytic materials adsorbed in the packed bed to vary the CO/CO₂ ratio, such as minerals containing calcium hydroxide [42]. On the other hand, CO₂ capture has been successfully proved at temperature ranges between 30 °C and 100 °C for silica-based adsorbents [59]. Moreover, low-temperature adsorption has also been achieved with ceramics [60]. Hence, it would be consistent to consider that it is also possible with zeolite-based materials (aluminosilicate-based substances as ceramics), as in this case. The temperature range achieved in the lower part of the packed bed shows that both catalytic reforming and CO₂ adsorption over zeolite are suitable in the operating conditions that were achieved. According to Cunha et al. [61], water conversion into hydrogen through steam gasification reactions start being verified at around 120 °C with nickel-based catalysts, even if full conversion would require temperatures in the range of 200 °C. Moreover, CO₂ adsorption over zeolite has also been reported at atmospheric pressure levels and temperature ranges around 100 °C. Zhao et al. [3], for instance, reported that zeolite can adsorb CO₂ over its surface with efficiencies above 5% under relatively low pressure and temperature levels. Considering such reported records together with the temperature registers, it is possible to affirm that the packed bed has activity in the syngas quality obtained from the gasifier. Such activity could be noticed due to the temperature drop registered during gasification. Even if the inner temperature sensor showed that it was possible to achieve temperature figures above 120 °C, the thermal images show that it dropped to approximately 33 °C in the upper sections of the packed bed. Even if this phenomenon can be related to the syngas shifting, it is affirmed that its specific performance requires further study.

Regarding the experimental oxygen contents, even if the energy carriers' content were increased in syngas, it is also shown that the remnant oxidizing agent is significant if compared with the reported results of other syngas quality improvement alternatives. This fact leads to the consideration that several operational parameters, such as oxygen feed and reflux ratio, need to be optimised in further studies and tests. From the chemical reaction engineering perspective, the reported operation could have been performed with an excess of one of the reactants, or the retention time could have been larger for increasing the conversion rate of oxygen. Hence, further experiments could consider a larger reflux ratio, which would imply a higher retention time; moreover, the effect of reducing the oxygen feed rate should be assessed for determining whether such variation affects the performance of the operation. It is also expected that a variation of this type enhances the obtained figures of cold gas efficiency in all cases, which is related to the energy vectors content increase [62].

Concerning the economic feasibility of the presented syngas improvement alternative, the relative costs figures show an increase of 4.3% if compared with a gasifier without the upper chamber required. In addition, CGE can be increased in at least 24.6% while CO/CO₂ ratio can be increased up to 3.5 times. Based on this figure and the above-mentioned effectiveness, it is possible to affirm that including a packed bed in the upper part of the gasifier is a suitable alternative that can be combined with other proposals without increasing the implementation costs. In addition, the link between performance and profitability [63] shows that the CGE improvement (achieved by including the upper packed bed in experimental assays) should be validated in real operation, based on the presented results.

5. Conclusions

Results showed that adding a packed bed as part of a gasifier is suitable as a low-complexity gas-shift alternative, since it was proved to perform correctly under atmospheric pressure conditions and in the absence of sophisticated auxiliary services, such as the gas compression facilities of moving bed gasification configurations. This was demonstrated by comparing the syngas composition of several gasification experimental experiences. The CGE of gasification could be increased by at least 24.6% without significantly compromising economic aspects or technical considerations.

Regarding the specific effect of the packed bed on syngas quality, it is noted that the obtained values of the CO/CO₂ ratio are shown to be remarkably higher than figures reported for other

gasification experimental experiences. Therefore, it can be suggested that the dominant effect of the packed-bed is CO₂ adsorption.

6. Patents

The patent entitled “Gasificador para mezclas de biomasa sólida con distintos contenidos de humedad” (IEPI MU 2016-185) is related to the work described in this document, and was granted by the Ecuadorian Patent Office in April 2016.

Acknowledgments: Authors thank the Secretary of Higher Education, Science, Technology and Innovation of Ecuador for financing the research project “MODELO CINÉTICO E IMPLEMENTACIÓN DE REACTOR PILOTO PARA COGASIFICACIÓN DE RESIDUOS SÓLIDOS Y CARBÓN VEGETAL PARA PRODUCCIÓN DE COMBUSTIBLES” under the grant agreement 20140122 CI.

Author Contributions: Ricardo A. Narváez C., Valeria Ramírez, and Diego Chulde conceived and designed the experiments; Diego Chulde performed the experimental assays in the pilot-scale facility; Valeria Ramírez performed the laboratory tests of biomass and prepared the comparison parameters presented in this article; Ricardo A. Narváez C., Roger Dixon, and Richard Blanchard analysed the data; and Ricardo A. Narváez C. and Richard Blanchard wrote the paper

Conflicts of Interest: The authors declare no conflict of interest.

References

1. Lugato, E.; Vaccari, F.P.; Genesio, L.; Baronti, S.; Pozzi, A.; Rack, M.; Woods, J.; Simonetti, G.; Montanarella, L.; Miglietta, F. An energy-biochar chain involving biomass gasification and rice cultivation in Northern Italy. *GCB Bioenergy* **2013**, *5*, 192–201. [[CrossRef](#)]
2. Masnadi, M.S.; Habibi, R.; Kopyscinski, J.; Hill, J.M.; Bi, X.; Lim, C.J.; Ellis, N.; Grace, J.R. Fuel characterization and co-pyrolysis kinetics of biomass and fossil fuels. *Fuel* **2014**, *117*, 1204–1214. [[CrossRef](#)]
3. Zhao, R.; Deng, S.; Wang, S.; Zhao, L.; Zhang, Y.; Liu, B.; Li, H.; Yu, Z. Thermodynamic research of adsorbent materials on energy efficiency of vacuum-pressure swing adsorption cycle for CO₂ capture. *Appl. Therm. Eng.* **2018**, *128*, 818–829. [[CrossRef](#)]
4. Jayathilake, R.; Rudra, S. Numerical and experimental investigation of Equivalence Ratio (ER) and feedstock particle size on birchwood gasification. *Energies* **2017**, *10*, 1232. [[CrossRef](#)]
5. Eri, Q.; Wu, W.; Zhao, X. Numerical Investigation of the Air-Steam Biomass Gasification Process Based on Thermodynamic Equilibrium Model. *Energies* **2017**, *10*, 2163. [[CrossRef](#)]
6. Caceres, E.; Alca, J.J. Rural Electrification Using Gasification Technology: Experiences and Perspectives. *IEEE Lat. Am. Trans.* **2016**, *14*, 3322–3328. [[CrossRef](#)]
7. Mahapatra, S.; Dasappa, S. Rural electrification: Optimising the choice between decentralised renewable energy sources and grid extension. *Energy Sustain. Dev.* **2012**, *16*, 146–154. [[CrossRef](#)]
8. Dasappa, S. Potential of biomass energy for electricity generation in sub-Saharan Africa. *Energy Sustain. Dev.* **2011**, *15*, 203–213. [[CrossRef](#)]
9. Kobayakawa, T.; Kandpal, T.C. Optimal resource integration in a decentralized renewable energy system: Assessment of the existing system and simulation for its expansion. *Energy Sustain. Dev.* **2016**, *34*, 20–29. [[CrossRef](#)]
10. Arpornwichanop, A.; Im-orb, K.; Simasatitkul, L. Techno-economic analysis of the biomass gasification and Fischer-Tropsch integrated process with off-gas recirculation. *Energy* **2016**, *94*, 483–496.
11. Tremel, A.; Becherer, D.; Fendt, S.; Gaderer, M.; Spliethoff, H. Performance of entrained flow and fluidised bed biomass gasifiers on different scales. *Energy Convers. Manag.* **2013**, *69*, 95–106. [[CrossRef](#)]
12. Morandin, M.; Maréchal, F.; Giacomini, S. Synthesis and thermo-economic design optimization of wood-gasifier-SOFC systems for small scale applications. *Biomass Bioenergy* **2013**, *49*, 299–314. [[CrossRef](#)]
13. Chaves, L.I.; da Silva, M.J.; de Souza, S.N.M.; Secco, D.; Rosa, H.A.; Nogueira, C.E.C.; Frigo, E.P. Small-scale power generation analysis: Downdraft gasifier coupled to engine generator set. *Renew. Sustain. Energy Rev.* **2016**, *58*, 491–498. [[CrossRef](#)]
14. Naqvi, M.; Yan, J.; Dahlquist, E.; Naqvi, S.R. Off-grid electricity generation using mixed biomass compost: A scenario-based study with sensitivity analysis. *Appl. Energy* **2017**, *201*, 363–370. [[CrossRef](#)]

15. Couto, N.D.; Silva, V.B.; Monteiro, E.; Rouboa, A.; Brito, P. An experimental and numerical study on the Miscanthus gasification by using a pilot scale gasifier. *Renew. Energy* **2017**, *109*, 248–261. [CrossRef]
16. Quintella, C.M.; Hatimondi, S.A.; Musse, A.P.S.; Miyazaki, S.F.; Cerqueira, G.S.; de Araujo Moreira, A. CO₂ capture technologies: An overview with technology assessment based on patents and articles. *Energy Procedia* **2011**, *4*, 2050–2057. [CrossRef]
17. Rackley, S.A. *Carbon Capture and Storage*; Butterworth-Heinemann: Oxford, UK, 2010.
18. Paolucci, M.; Filippis, P.D.; Borgianni, C. Pyrolysis and Gasification of Municipal and Industrial wastes blends. *Therm. Sci.* **2010**, *14*, 739–746. [CrossRef]
19. Narváez C., R.A. Gasificador Para Mezclas de Biomasa Sólida con Distintos Contenidos de Humedad. IEPI MU 2016-185. 2016. Available online: https://lunet-my.sharepoint.com/:b:/r/personal/elran_lunet_lboro_ac_uk/Documents/expediente_patente.pdf?csf=1&e=8gLpFO (accessed on 25 January 2018).
20. Chianese, S.; Loipersböck, J.; Malits, M.; Rauch, R.; Hofbauer, H.; Molino, A.; Musmarra, D. Hydrogen from the high temperature water gas shift reaction with an industrial Fe/Cr catalyst using biomass gasification tar rich synthesis gas. *Fuel Process. Technol.* **2015**, *132*, 39–48. [CrossRef]
21. Hla, S.S.; Morpeth, L.D.; Dolan, M.D. Modelling and experimental studies of a water–gas shift catalytic membrane reactor. *Chem. Eng. J.* **2015**, *276*, 289–302. [CrossRef]
22. Kumagai, S.; Alvarez, J.; Blanco, P.H.; Wu, C.; Yoshioka, T.; Olazar, M.; Williams, P.T. Novel Ni-Mg-Al-Ca catalyst for enhanced hydrogen production for the pyrolysis-gasification of a biomass/plastic mixture. *J. Anal. Appl. Pyrolysis* **2015**, *113*, 15–21. [CrossRef]
23. Chianese, S.; Fail, S.; Binder, M.; Rauch, R.; Hofbauer, H.; Molino, A.; Blasi, A.; Musmarra, D. Experimental investigations of hydrogen production from CO catalytic conversion of tar rich syngas by biomass gasification. *Catal. Today* **2016**, *277*, 182–191. [CrossRef]
24. Dongil, A.B.; Pastor-Pérez, L.; Escalona, N.; Sepúlveda-Escribano, A. Carbon nanotube-supported Ni-CeO₂ catalysts. Effect of the support on the catalytic performance in the low-temperature WGS reaction. *Carbon* **2016**, *101*, 296–304. [CrossRef]
25. Wang, C.; Liu, C.; Fu, W.; Bao, Z.; Zhang, J.; Ding, W.; Chou, K.; Li, Q. The water-gas shift reaction for hydrogen production from coke oven gas over Cu/ZnO/Al₂O₃ catalyst. *Catal. Today* **2016**, *263*, 46–51. [CrossRef]
26. Keskin, S.; Van Heest, T.; Sholl, D. Can Metal-Organic Framework Materials Play a Useful Role in Large-Scale Carbon Dioxide Separations. *ChemSusChem* **2010**, *3*, 879–891. [CrossRef] [PubMed]
27. Campo, M.C.; Ribeiro, A.M.; Ferreira, A.F.P.; Santos, J.C.; Lutz, C.; Loureiro, J.M.; Rodrigues, A.E. Carbon dioxide removal for methane upgrade by a VSA process using an improved 13X zeolite. *Fuel Process. Technol.* **2016**, *143*, 185–194. [CrossRef]
28. Basu, P. *Biomass Gasification, Pyrolysis and Torrefaction*, 2nd ed.; Academic Press: San Diego, MA, USA, 2013.
29. Liu, L.; Zhao, C.; Xu, J.; Li, Y. Integrated CO₂ capture and photocatalytic conversion by a hybrid adsorbent/photocatalyst material. *Appl. Catal. B Environ.* **2015**, *179*, 489–499. [CrossRef]
30. Ravaghi-Ardebili, Z.; Manenti, F.; Pirola, C.; Soares, F.; Corbetta, M.; Pierucci, S.; Ranzi, E. Influence of the Effective Parameters on H₂:CO Ratio of Syngas at Low-Temperature Gasification. *Chem. Eng. Trans.* **2014**, *37*, 253–258.
31. Sagüés, C.; García-Bacaicoa, P.; Serrano, S. Automatic control of biomass gasifiers using fuzzy inference systems. *Bioresour. Technol.* **2007**, *98*, 845–855. [CrossRef] [PubMed]
32. Izquierdo, U.; Barrio, V.L.; Bizkarra, K.; Gutierrez, A.M.; Arraibi, J.R.; Gartzia, L.; Bañuelos, J.; Lopez-Arbeloa, I.; Cambra, J.F. Ni and RhNi catalysts supported on Zeolites L for hydrogen and syngas production by biogas reforming processes. *Chem. Eng. J.* **2014**, *238*, 178–188. [CrossRef]
33. Fakeeha, A.H.; Al-Fatesh, A.S.; Abasaeed, A.E. Stabilities of zeolite-supported Ni catalysts for dry reforming of methane. *Chin. J. Catal.* **2013**, *34*, 764–768. [CrossRef]
34. Kacem, M.; Pellerano, M.; Delebarre, A. Pressure swing adsorption for CO₂/N₂ and CO₂/CH₄ separation: Comparison between activated carbons and zeolites performances. *Fuel Process. Technol.* **2015**, *138*, 271–283. [CrossRef]
35. Tsunogi, N.; Yuki, S.; Oumi, Y.; Sekikawa, M.; Sasaki, Y.; Sadakane, M.; Sano, T. Design of Microporous Material HUS-10 with Tunable Hydrophilicity, Molecular Sieving, and CO₂ Adsorption Ability Derived from Interlayer Silylation of Layered Silicate HUS-2. *ACS Appl. Mater. Interfaces* **2015**, *7*, 24360–24369. [CrossRef] [PubMed]

36. Molino, A.; Iovane, P.; Donatelli, A.; Braccio, G.; Chianese, S.; Musmarra, D. Steam Gasification of Refuse-Derived Fuel in a Rotary Kiln Pilot Plant: Experimental Tests. *Chem. Eng. Trans.* **2013**, *32*. [[CrossRef](#)]
37. González-Vázquez, M.P.; García, R.; Pevida, C.; Rubiera, F. Optimization of a Bubbling Fluidized Bed Plant for Low-Temperature Gasification of Biomass. *Energies* **2017**, *10*, 306. [[CrossRef](#)]
38. Qadi, N.M.; Zaini, I.N.; Takahashi, F.; Yoshikawa, K. CO₂ cogasification of coal and algae in a downdraft fixed-bed gasifier: Effect of CO₂ partial pressure and blending ratio. *Energy Fuels* **2017**, *31*, 2927–2933. [[CrossRef](#)]
39. Lapuerta, M.; Hernández, J.J.; Pazo, A.; López, J. Gasification and co-gasification of biomass wastes: Effect of the biomass origin and the gasifier operating conditions. *Fuel Process. Technol.* **2008**, *89*, 828–837. [[CrossRef](#)]
40. Vladan, S.; Jinescu, G. The Production of a Fuel Gas with High Content of Hydrogen through Biomass Gasification. *Rev. Chim.* **2010**, *61*, 1223–1225.
41. Rizkiana, J.; Guan, G.; Widayatno, W.B.; Hao, X.; Huang, W.; Tsutsumi, A.; Abudula, A. Effect of biomass type on the performance of cogasification of low rank coal with biomass at relatively low temperatures. *Fuel* **2014**, *134*, 414–419. [[CrossRef](#)]
42. Liu, Y.; Liu, L.; Hong, L. Gasification of char with CO₂ to produce CO—Impact of catalyst carbon interface. *Catal. Today* **2017**, *281*, 352–359. [[CrossRef](#)]
43. Smoliński, A.; Howaniec, N. Co-gasification of coal/sewage sludge blends to hydrogen-rich gas with the application of simulated high temperature reactor excess heat. *Int. J. Hydrogen Energy* **2016**, *41*, 8154–8158. [[CrossRef](#)]
44. Howaniec, N.; Smoliński, A. Influence of fuel blend ash components on steam co-gasification of coal and biomass—Chemometric study. *Energy* **2014**, *78*, 814–825. [[CrossRef](#)]
45. NORDTEST. NT ENVIR 001—Solid Waste, Municipal: Sampling and Characterization, 1st ed.; NORDTEST: Espoo, Finland, 1995.
46. Perez, D.D.S.; Dupont, C.; Guillemain, A.; Jacob, S.; Labalette, F.; Briand, S.; Marsac, S.; Guerrini, O.; Broust, F.; Commandre, J.M. Characterisation of the Most Representative Agricultural and Forestry Biomasses in France for Gasification. *Waste Biomass Valoriz.* **2015**, *6*, 515–526. [[CrossRef](#)]
47. Atnaw, S.M.; Sulaiman, S.A.; Yusup, S. Influence of fuel moisture content and reactor temperature on the calorific value of syngas resulted from gasification of oil palm fronds. *Sci. World J.* **2014**, *2014*, 121908. [[CrossRef](#)] [[PubMed](#)]
48. D’orazio, A.; Rapagnà, S.; Foscolo, P.U.; Gallucci, K.; Nacken, M.; Heidenreich, S.; Di Carlo, A.; Dell’Era, A. Gas conditioning in H₂ rich syngas production by biomass steam gasification: Experimental comparison between three innovative ceramic filter candles. *Int. J. Hydrogen Energy* **2015**, *40*, 7282–7290. [[CrossRef](#)]
49. Wang, Z.; Wang, Z.; He, T.; Qin, J.; Wu, J.; Li, J.; Zi, Z.; Liu, G.; Wu, J.; Sun, L. Gasification of biomass with oxygen-enriched air in a pilot scale two-stage gasifier. *Fuel* **2015**, *150*, 386–393. [[CrossRef](#)]
50. Ju, Y.; Lee, C.H. Evaluation of the energy efficiency of the shell coal gasification process by coal type. *Energy Convers. Manag.* **2017**, *143*, 123–136. [[CrossRef](#)]
51. Howaniec, N.; Smoliński, A. Effect of fuel blend composition on the efficiency of hydrogen-rich gas production in co-gasification of coal and biomass. *Fuel* **2014**, *128*, 442–450. [[CrossRef](#)]
52. Kaewluan, S.; Pipatmanomai, S. Gasification of high moisture rubber woodchip with rubber waste in a bubbling fluidized bed. *Fuel Process. Technol.* **2011**, *92*, 671–677. [[CrossRef](#)]
53. Nam, H.; Maglinao, A.L.; Capareda, S.C.; Rodriguez-Alejandro, D.A. Enriched-air fluidized bed gasification using bench and pilot scale reactors of dairy manure with sand bedding based on response surface methods. *Energy* **2016**, *95*, 187–199. [[CrossRef](#)]
54. Pangarkar, K.; Schildhauer, T.J.; van Ommen, J.R.; Nijenhuis, J.; Kapteijn, F.; Moulijn, J.A. Structured packings for multiphase catalytic reactors. *Ind. Eng. Chem. Res.* **2008**, *47*, 3720–3751. [[CrossRef](#)]
55. Boyes, A.P.; Lu, X.X.; Raymahasay, S.; Saremento, S.; Tilston, M.W.; Winterbottom, J.M. The cocurrent downflow contactor (CDC): Mass-transfer and reaction characteristics in unpacked and packed-bed operation. *Chem. Eng. Res. Des.* **1991**, *69*, 200–202.
56. Shen, Y.; Chen, M.; Sun, T.; Jia, J. Catalytic reforming of pyrolysis tar over metallic nickel nanoparticles embedded in pyrochar. *Fuel* **2015**, *159*, 570–579. [[CrossRef](#)]
57. Bakhtiari, M.; Zahid, M.A.; Ibrahim, H.; Khan, A.; Sengupta, P.; Idem, R. Oxygenated hydrocarbons steam reforming over Ni/CeZrGdO₂ catalyst: Kinetics and reactor modeling. *Chem. Eng. Sci.* **2015**, *138*, 363–374. [[CrossRef](#)]

58. Hamad, M.A.; Radwan, A.M.; Heggo, D.A.; Moustafa, T. Hydrogen rich gas production from catalytic gasification of biomass. *Renew. Energy* **2016**, *85*, 1290–1300. [[CrossRef](#)]
59. Goel, C.; Bhunia, H.; Bajpai, P.K. Development of nitrogen enriched nanostructured carbon adsorbents for CO₂ capture. *J. Environ. Manag.* **2015**, *162*, 20–29. [[CrossRef](#)] [[PubMed](#)]
60. Sarma, H.; Ogunwumi, S. Novel Low Temperature Ceramics for CO₂ Capture. In *Advances in Bioceramics and Porous Ceramics VII: A Collection of Papers, Presented at the 38th International Conference on Advanced Ceramics and Composites, Daytona Beach, FL, USA, 27–31 January 2015*; John Wiley & Sons: Hoboken, NJ, USA, 2015; pp. 165–172.
61. Cunha, A.F.; Moreira, M.N.; Mafalda Ribeiro, A.; Ferreira, A.P.; Loureiro, J.M.; Rodrigues, A.E. How to Overcome the Water-Gas-Shift Equilibrium using a Conventional Nickel Reformer Catalyst. *Energy Technol.* **2015**, *3*, 1205–1216. [[CrossRef](#)]
62. Tamosiunas, A.; Chouchene, A.; Valatkevičius, P.; Jeguirim, M. The potential of thermal plasma gasification of olive pomace charcoal. *Energies* **2017**, *10*, 710. [[CrossRef](#)]
63. Borello, D.; Pantaleo, A.M.; Caucci, M.; Caprariis, B.D.; Filippis, P.D.; Shah, N. Modeling and experimental study of a small scale olive pomace gasifier for cogeneration: Energy and profitability analysis. *Energies* **2017**, *10*, 1930. [[CrossRef](#)]



© 2018 by the authors. Licensee MDPI, Basel, Switzerland. This article is an open access article distributed under the terms and conditions of the Creative Commons Attribution (CC BY) license (<http://creativecommons.org/licenses/by/4.0/>).